



## Investigation on Saprolitic Laterite Ore Reduction Process using Palm Kernel Shell Charcoal: Kinetics and Phase Transformation

Himawan Tri Bayu Murti Petrus<sup>1,2\*</sup>, Andreas Diga Pratama Putera<sup>1</sup>, I Wayan Warmada<sup>2,3</sup>, Fajar Nurjaman<sup>4</sup>, Widi Astuti<sup>4</sup>, Agus Prasetya<sup>1,2</sup>

<sup>1</sup>Department of Chemical Engineering (Sustainable Mineral Processing Research Group), Faculty of Engineering, Universitas Gadjah Mada, Jl. Grafika No. 2, Yogyakarta 55281, Indonesia

<sup>2</sup>Unconventional Geo-resources Research Center, Faculty of Engineering, Universitas Gadjah Mada, Jl. Grafika No. 2, Yogyakarta 55281, Indonesia

<sup>3</sup>Department of Geological Engineering, Faculty of Engineering, Universitas Gadjah Mada, Jl. Grafika No. 2, Yogyakarta 55281, Indonesia

<sup>4</sup>Research Unit for Mineral Technology, Indonesian Institute of Sciences (LIPI), Jl. Ir. Sutami Km. 15, Tanjung Bintang, Lampung Selatan, Indonesia

**Abstract.** The performance and kinetic of saprolitic laterite reduction using palm kernel shell charcoal and anthracite were studied. The anthracite coal represents the conventional high-grade carbon content matter, and palm kernel shell charcoal represents biomass-based reductant. The experiment was conducted at a temperature ranging from 800°C and 1000°C. XRD analysis was applied to observe phase transformation. For the kinetic study, two models, namely (1) Jander and (2) Ginstling-Brounstein diffusion model, were applied. The mineral phase results indicated that both reductants yield Magnetite from Goethite in the laterite. The best fit model is obtained by the Jander model with the energy activation of 33.68 kJ/mol for anthracite reductant and 10.99 – 18.19 kJ/mol for palm kernel shell reductant, indicating that reduction is easier to occur using palm kernel shell.

**Keywords:** Kinetics; Phase transformation; Reduction; Roasting; Saprolite

### 1. Introduction

Nickel could be a transition component with properties of ferrous and nonferrous metals (Kim et al., 2010). Nickel ore is affiliated with oxide (nickel laterite) or sulfur (nickel sulfide). Almost 58% of nickel requests are provided by sulfide metals, even though 78% of nickel is stored in laterite minerals (Dalvi et al., 2004). However, as the continuous exploitation of sulphidic ores occurred in recent years, the sources became scarce and underground mining was introduced. Consequently, the exploitation cost was rising, especially the labour cost. On the contrary, the mining activity of laterite deposits is considerably shallow (usually less than 50 meters) (Elias, 2002). So, much concern has been concentrated on using low-grade nickel ore (especially those containing <2.0 wt.% nickel) (Lee et al., 2005), such as laterites.

In terms of nickel laterite, Indonesia has an abundant deposit of it. About 12% of nickel

\*Corresponding author's email: [bayupetrus@ugm.ac.id](mailto:bayupetrus@ugm.ac.id), Tel/Fax.: +62-0274-555320

doi: [10.14716/ijtech.v13i3.4701](https://doi.org/10.14716/ijtech.v13i3.4701)

laterite resources are stored in Indonesia (Dalvi et al., 2004). Until 2013, Indonesia is one of the biggest nickel mine producers. However, the Government issued a new policy to limit direct export activities to encourage the production of ferronickel and nickel pig iron (U.S. Geological Survey, 2014). This condition pushes stakeholders, industries, and researchers to develop nickel laterite processing in Indonesia.

There are two kinds of laterite, namely limonite and saprolite. Limonite is low-nickel content laterite (around 0.8-1.5% Ni-mass), and saprolite is a rich-nickel content (more than 1.5-3% Ni-mass) (Whittington & Muir, 2000). Both hydrometallurgical and pyrometallurgical processes can be used to extract nickel from the laterites. However, due to its high nickel content, saprolite ore is better processed by pyrometallurgy (Li et al., 2011; Minister of Energy and Mineral Resources Republic of Indonesia, 2013). There are usually three unit operations in the pyrometallurgical process: roasting, smelting, and converting. The reduction process consumes carbon-based reductant, usually coke, and produces a tremendous amount of carbon dioxide. This process is highly energy-consuming (Guo et al., 2009) and not environmentally friendly. Replacing the coke with bio-reductant has been an interesting issue concerning carbon dioxide emission to be studied.

The works done to study the possibility of using bio-reductants in the process with attention to some parameters are limited. Chen et al. (2015) suggested that bio-coal reductants can be used to reduce the major phase in the limonitic laterite ore ( $\text{Fe}_{1.833}(\text{OH})_{0.5}\text{O}_{2.5}$  and  $\text{Fe}_2\text{SiO}_4$ ) into a metal phase, such as Fe,  $\text{Fe}_{0.64}\text{Ni}_{0.36}$ . Yunus et al. (2014) suggested that empty fruit bunch derived bio-char can upgrade the magnetic properties of goethite-rich iron ore by temperature dependence serial reduction process of hematite ( $\text{Fe}_2\text{O}_3$ ), magnetite ( $\text{Fe}_3\text{O}_4$ ), and wustite ( $\text{FeO}$ ). However, there is still no evidence explaining the corresponding phenomena other than the equilibrium explanation. To the best of knowledge, there are still few works on kinetics and phase transformation study studies in the pyrometallurgy process using biomass-based reductants, which are critical for the scaling-up phase in the industry.

Following 'Indonesia's target to export a minimum nickel content of 4.0%, developing a nickel laterite processing plant in the country is necessary. To support the idea, a study confirms that Ni content in Fe-Ni alloy from lateritic sources can reach 4.5% (Citrawati et al., 2020). The latest research concerning the phase transformation and kinetics study uses coconut shell and lamtoro (*Leucaena leucocephala*) charcoal as reductants. It proves that the biomass-based charcoal could be a good substitute the conventional coal in the roasting process of nickel laterite. Both studies yield magnetite ( $\text{Fe}_3\text{O}_4$ ) with identical kinetics parameters, leading to the conventional coal, leading to a good step for the biomass-based charcoal to substitute the conventional coal (Petrus et al., 2017; Putera et al., 2017).

The main goals of the current work are to provide detailed qualitative and quantitative information on phase transformation and the reduction mechanism of saprolitic laterite ore reduction with palm kernel shell charcoal. Phase transformation is important to be studied, especially in Iron and Nickel, because the expected end-product is nickel pig iron, a cheaper alternative to pure nickel for stainless steel production (low-grade ferronickel) (Petrus et al., 2016). Knowing the kinetics parameter of the biomass-based reductant (palm kernel shell charcoal), the scaling up of the sustainable technique in saprolitic laterite ore through a pyrometallurgical approach can be established.

## 2. Methods

### 2.1. Raw Materials Characterization

Saprolitic laterite ore was collected from Pomalaa, Southeast Sulawesi, Indonesia. The sample was mineralogically and chemically characterized. X-ray fluorescence (XRF, ZSX

Primus II, Rigaku, Tokyo, Japan) was used to determine the chemical composition. The sample was found to have high iron, magnesium, silica, and nickel contents, as shown in Table 1. The phase transformation process in the reduction process was assessed by XRD using an X-ray diffractometer (XRD, Ultima IV, Rigaku, Tokyo, Japan) with Cu-K $\alpha$  radiation ( $\lambda=1.5418 \text{ \AA}$ ) between 5° and 65°, and a scanning step of 0.02 in 2 $\theta$  (degree). The saprolitic laterite ore XRD result is shown in Figure 1, and serpentine (Mg<sub>3</sub>Si<sub>2</sub>O<sub>5</sub>(OH)<sub>4</sub>) and Goethite (Fe-OOH) were found to be the predominant minerals. Nickel only presents in small quantities in this research and is usually associated with the iron (Rasyid et al., 2016) and silicate groups (olivine and serpentine) (Ribeiro et al., 2019).

**Table 1** Saprolite chemical elemental and corresponding oxide composition

Elements	wt.%	Oxides	wt.%
O	38.00		
Fe	32.39	Fe <sub>2</sub> O <sub>3</sub>	46.30
Si	13.82	SiO <sub>2</sub>	29.57
Mg	6.69	MgO	11.10
Ni	3.90	NiO	4.97
Al	1.49	Al <sub>2</sub> O <sub>3</sub>	2.81
Cr	1.21	Cr <sub>2</sub> O <sub>3</sub>	1.77
Ca	0.71	CaO	1.00
Mn	0.60	MnO	0.78
Co	0.18	CoO	0.23
K	0.17	K <sub>2</sub> O	0.20

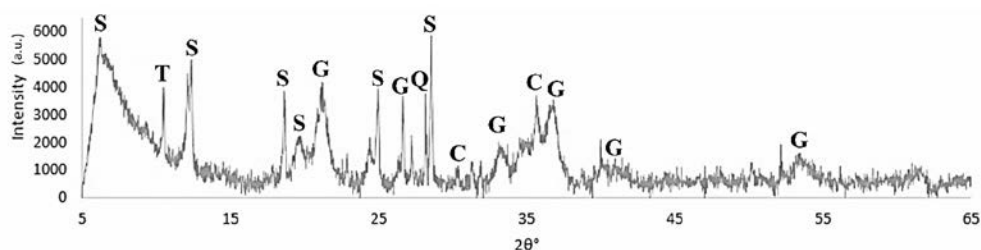


**Figure 1** XRD pattern of raw saprolite ore. [S: serpentine (Mg<sub>3</sub>Si<sub>2</sub>O<sub>5</sub>(OH)<sub>4</sub>); T: talc (Mg<sub>3</sub>Si<sub>4</sub>O<sub>10</sub>(OH)<sub>2</sub>); G: goethite (FeOOH); Q: quartz (SiO<sub>2</sub>); C: chromite (FeCr<sub>2</sub>O<sub>4</sub>)]. Source: (Petrus et al., 2017)

Two reductants, anthracite coal from Painan, West Sumatra, Indonesia, and palm kernel shell charcoal, were characterized using proximate analysis, as shown in Table 2.

**Table 2** Proximate analysis results of the reductants

Reductant	Ash Content [wt.%]	Moisture Content [wt.%]	Volatile Matter [wt.%]	Fixed Carbon [wt.%]
Anthracite Coal	2.50	2.30	7.40	87.90
Palm kernel shell charcoal	3.70	6.00	13.20	77.20

### 2.2. Experiment

Before the reduction roasting process, palm kernel shell charcoal, anthracite coal, and saprolite ore were grounded and screened to get the desired size (-100+120 mesh). The powders were collected and then mixed with water in a specific composition, as shown in Table 3, to form pellets with hands. The pellets were dried at 110°C for 4 hours to remove the moisture content.

For all specimens shown in Table 3, the pellets were placed in a 20 mL half-cylinder ceramic crucible. Each crucible contains two pellets, so the pellets are piled up. The 'pellets' mass is calculated before and after the roasting process. In the roasting process, three

isothermal stages of 800°C, 900°C, and 1000°C temperature were conducted in a muffle furnace. The pellets were inserted into the muffle furnace when the temperature reached the targets.

When the pellets reach the time targets, the crucibles are taken directly from the muffle furnace and then closed using the crucible's cap to prevent re-oxidation of the pellets. The crucibles are placed on steel to accelerate the cooling rate. The sample's name and compositions are shown in Table 3 below. *S* represents saprolite, *A* represents anthracite, and *PKS* represents palm kernel shell. The whole framework of the methodology is presented in Figure 2.

**Table 3** Samples name and compositions in the roasting experiment (g)

Name	Specimens		
	Saprolite	Anthracite coal	Palm kernel shell charcoal
S-A	4.00	1.00	-
S-PKS-a	4.00	-	1.00
S-PKS-b	3.75	-	1.25

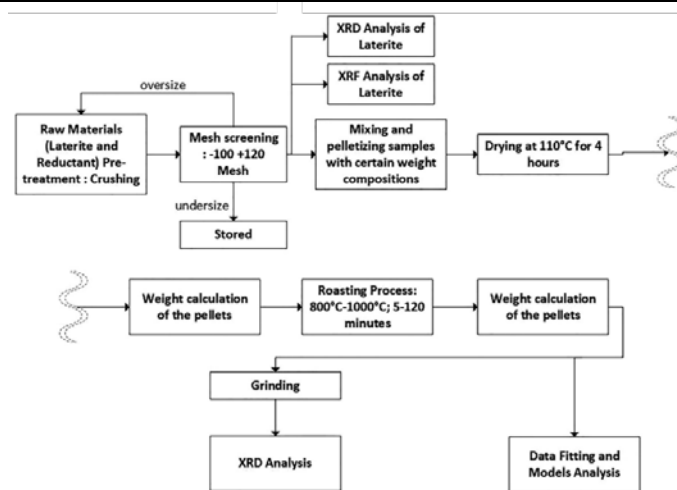


**Figure 2** Methodology framework

### 3. Results and Discussion

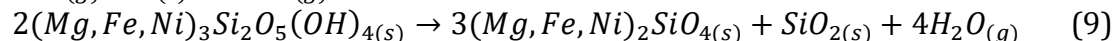
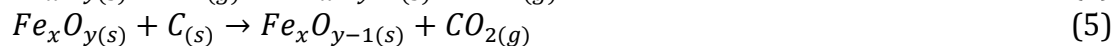
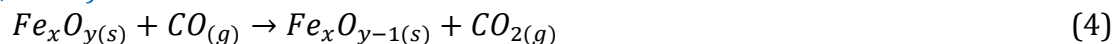
#### 3.1. Percentage of reduction

The percentage of the 'laterite's reduction is determined by gravimetry calculated from the mass loss of the samples. The mass loss represents the volatile matter, oxides leaving iron and nickel oxides, and carbon burned in the pellets. It is assumed that ash from the reductants will always remain in the pellet. The percentage of reduction is obtained from the mass loss of the samples in each measured time divided by the maximum mass loss (Khawam & Flanagan, 2006). The maximum mass loss of the samples is measured using the same method in the previous study by Petrus et al. (2019).

#### 3.2. Reduction mechanism

Previous studies agreed that the general reduction reactions are carried out by carbon monoxide, and thus, the reactions occur between solid metal oxides and gas. However, the carbon monoxide is obtained from the Boudouard reaction, which needs a high temperature (>1000°C) to yield mostly carbon monoxide in the C-CO-CO<sub>2</sub> system (Fu et al., 2012; Li et al., 2013). Other than this condition, metal oxides reduced by solid carbon prevail (Fu et al., 2012). Both direct and indirect reactions for iron and nickel are presented in equations (4) to (7). Regarding phase transformation of the Fe-bearing minerals, nickel reduction starts from serpentine transformation into olivine (Equation 9). Thus the

possible involving reactions proposed in this study are (Fu et al., 2012; Li et al., 2013; Petrus et al., 2019):



### 3.3. Reduction mechanism

Figure 3 below shows the percentage of reduction achieved from the gravimetry method by Petrus et al. (2019).

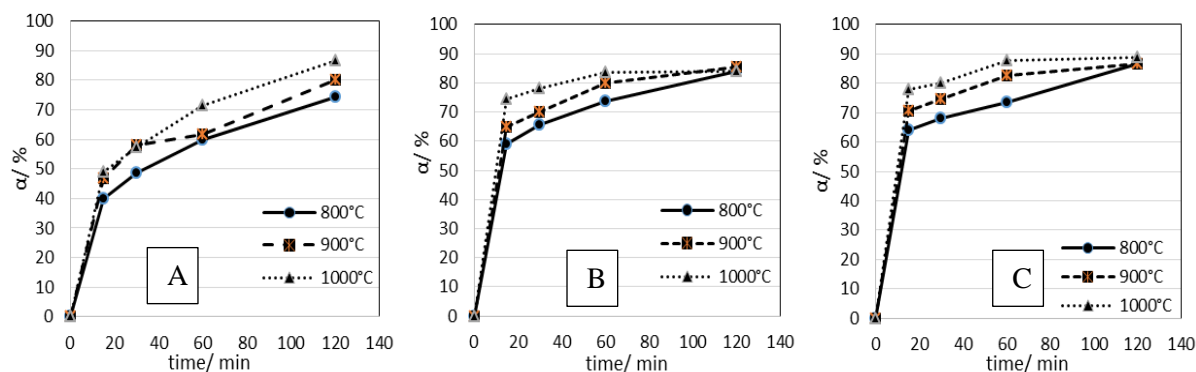


**Figure 3** Percentages of reduction of sample (A) S-A, (B) S-PKS-a, and (C) S-PKS-b

As reactions (4) and (6) are indirect reactions, the mechanism is different from reactions (5) and (7) that follow the direct reaction. In indirect reactions, the rate is controlled by the reaction step. The model is known as the first-order irreversible rate kinetics (Mondal et al., 2004). In direct reactions, the rate is controlled by a diffusion mechanism. The diffusion occurs between two contacting solids and a product layer between them. The rate of product formation decreases proportionally with the increased thickness of the product barrier layer. There are two forms of model equations depending on the layer's geometry. A flat barrier layer model is known as the Jander equation, and a spherical one is known as the Ginstling-Brounshtein equation (Khawam & Flanagan, 2006). The models are formulated following equations 10 and 11:

(a) Jander equation

$$f(\alpha) = \left(1 - (1 - \alpha)^{\frac{1}{3}}\right)^2 = k.t \tag{10}$$

(b) Ginstling-Brounshtein equation

$$f(\alpha) = 1 - \frac{2\alpha}{3} - (1 - \alpha)^{\frac{2}{3}} = k.t \tag{11}$$

Where  $\alpha$  is the percentage of mass loss of the sample (Petrus et al., 2019),  $k$  corresponds to the rate constant and follows Arrhenius equation  $k=A.exp(-E/RT)$ ,  $E$  and  $A$  represent the activation energy and pre-exponential factor.

### 3.4. Data fitting results

#### 3.4.1. Anthracite reductant

The reduction roasting process of saprolite with anthracite coal follows both Jander and Ginstling-Brounshtein equation accurately. The average correlation coefficients attained in the least square fitting are as significant as 0.9843 and 0.9646, respectively, indicating that the geometric of the 'particles' surface can be seen as either flat or spherical.

This might occur because the thickness of the barrier layer is significantly smaller than the size of the particles.

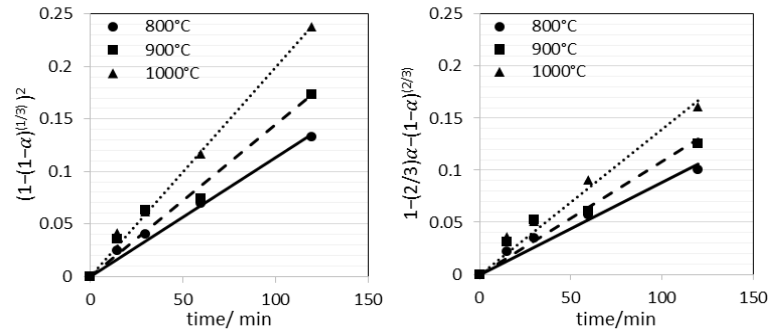


**Figure 4** Percentage of reduction data fitting with Jander and Ginstling-Brounshtein equation of S-A sample

The excellent agreement with the corresponding models represents that the direct reaction prevails. This finding agrees with the previous study by Fu et al. (Fu et al. 2012), which suggested that direct reduction will prevail below 1100°C. Furthermore, the kinetics parameters found in this mechanism are shown in Figure 5 and table 4 below.

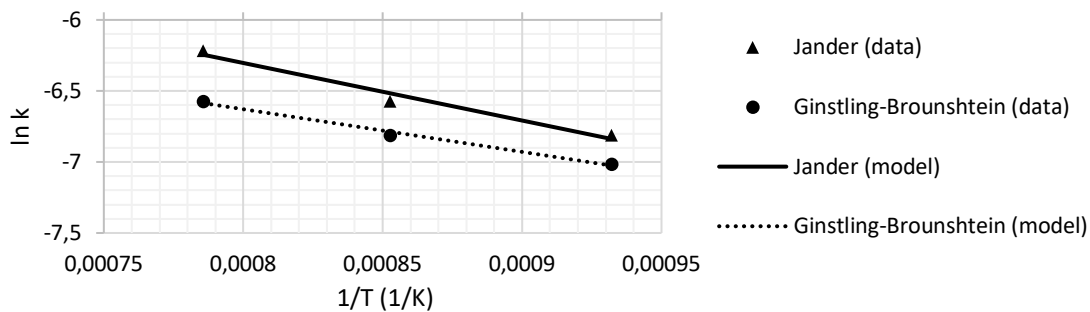


**Figure 5** Kinetics parameter correlation for S-A sample

**Table 4** Kinetics parameter of sample S-A

Model	E (kJoule/mol)	A (min <sup>-1</sup> )
Jander	33.68	467.66x10 <sup>-4</sup>
Ginstling-Brounshtein	24.96	145.99x10 <sup>-4</sup>

### 3.4.2. Palm kernel shell charcoal reductant

The fitting result of biomass-based reductant samples was not as good as the anthracite. The reaction tends to be very fast in the first 15 minutes, as shown in Figure 3 (b) and (c). This was due to the 'biomass's high volatile matter content, such as CH<sub>4</sub> (Kartohardjono et al., 2019), which is much more reactive and easy to evaporate, leading to a much faster reduction reaction in early time. The R-squared values for the fitting in the first sample (S-PKS-a) are 0.6273 and 0.5898, and for the second samples (S-PKS-b) are 0.6261 and 0.5895 for Jander and Ginstling-Brounshtein equation, respectively. Regardless of their values, both Jander and Ginstling-Brounshtein models own comparable R-squared. Again, this indicates that 'particles' surface can be flat or spherical.

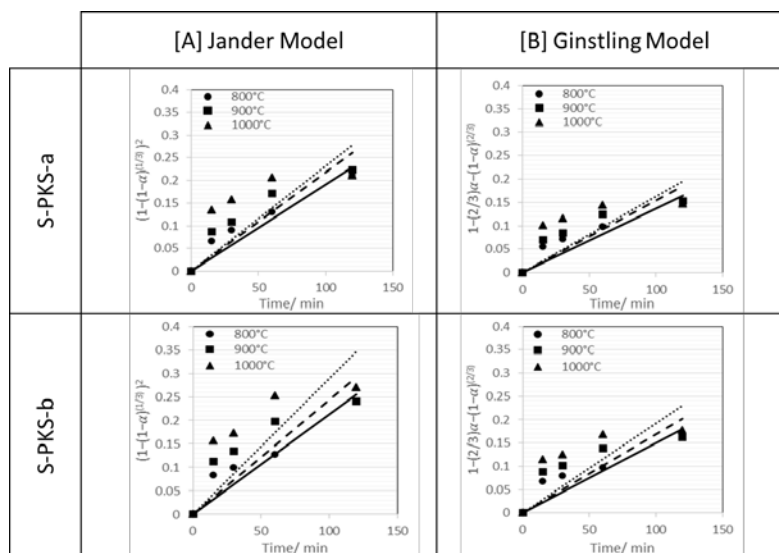


**Figure 6** Percentage of reduction data fitting with (A) Jander and (B) Ginstling-Brounshtein equation for S-PKS-a sample and S-PKS-b sample

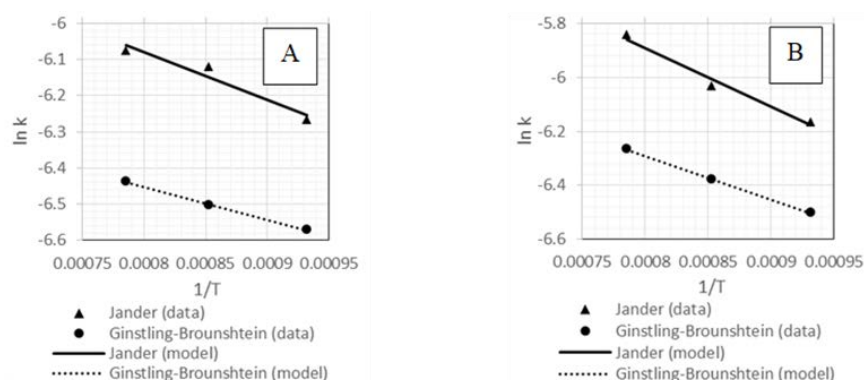


**Figure 7** Kinetics parameter correlation for (A) S-PKS-a and (B) S-PKS-b sample.

Having the kinetics parameters as shown in Tables 4 and 5, the palm kernel shell charcoal possesses appropriate characteristics to be applied in the reduction process of Indonesian saprolitic laterite ore with a lower value of activation energy than that of the anthracite reductant.

**Table 5** Kinetics parameter of bio-reductant samples (S-PKS-a and S-PKS-b)

Sample	Model	-E (kJoule/mol)	A (min <sup>-1</sup> )
S-PKS-a	Jander	10.99	65.96x10 <sup>-4</sup>
	Ginstling-Brounshtein	7.57	32.68x10 <sup>-4</sup>
S-PKS-b	Jander	18.19	159.39x10 <sup>-4</sup>
	Ginstling-Brounshtein	13.41	67.58x10 <sup>-4</sup>

### 3.5. Phase transformation

The phase transformation of the sample with anthracite reductant has been studied by Putera et al. (2017). It is found that magnetite, olivine, hematite, and quartz are present in the XRD result. In addition, magnetite peaks intensify at higher temperatures and longer reduction time (Putera *et al.*, 2017). In this research, the phase transformation of biomass-based reductant sample (S-PKS-a) in the roasting process of 1000°C is shown in Figure 8 below. According to the XRD analysis, the sample peaks are magnetite, olivine, hematite, and quartz (Rhamdhani et al., 2009). Magnetite peaks in the 2θ (degree) of 30.80, 35.80,

43.50, 54.10, 57.40, and 63.10 are the main constituent found in the roasted samples. With the increasing time of the reduction process, the peaks become more vivid with higher intensity, representing that the sample has a higher conversion of iron to form magnetite, which agrees with the previous study.

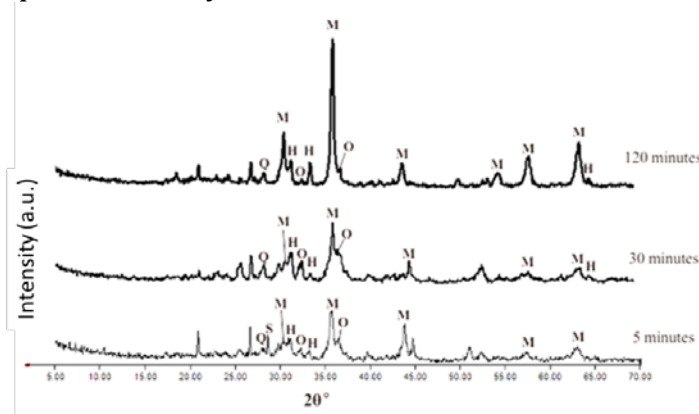


**Figure 8** XRD pattern of S-PKS-a sample in different times of reduction. [Q: quartz (SiO<sub>2</sub>); S: serpentine (Mg<sub>3</sub>Si<sub>2</sub>O<sub>5</sub>(OH)<sub>4</sub>); M: magnetite((Fe,Ni)O.Fe<sub>2</sub>O<sub>3</sub>); H: hematite (Fe<sub>2</sub>O<sub>3</sub>); O: Olivine ((Mg,Fe,Ni)<sub>2</sub>SiO<sub>4</sub>)]

In terms of temperature, as shown in Fig. 9, there are some significant differences between the crystal formed in the sample with 800, 900, and 1000°C reduction temperatures. Talc, quartz and serpentine exist at a reduction temperature of 800°C. Moreover, the lowest peak intensities of magnetite are found in the corresponding sample, showing the lowest conversion. However, wustite is not found in all result samples, possibly because the experiment temperatures are below metallization temperature at 1100°C (Oediyani et al., 2016). A higher temperature yields higher intensity of magnetite peaks, representing the higher conversion of iron reduction as formulated in equations 12 and 13 (Oediyani et al.,2016):

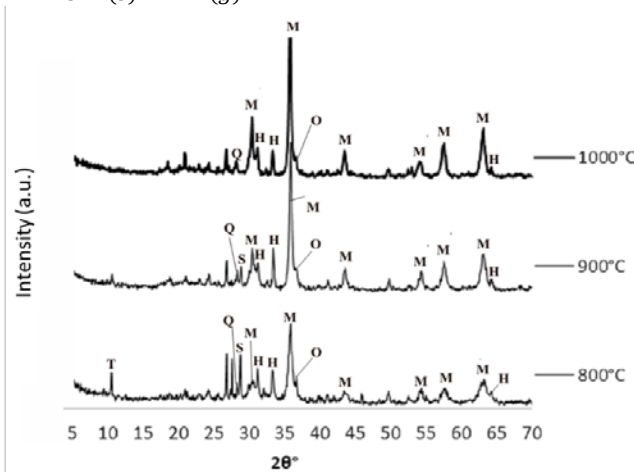


**Figure 9** XRD pattern of S-PKS-a sample in different temperatures. [T: talc (Mg<sub>3</sub>Si<sub>4</sub>O<sub>10</sub>(OH)<sub>2</sub>); Q: quartz (SiO<sub>2</sub>); S: serpentine (Mg<sub>3</sub>Si<sub>2</sub>O<sub>5</sub>(OH)<sub>4</sub>); M: magnetite((Fe,Ni)O.Fe<sub>2</sub>O<sub>3</sub>); H: hematite (Fe<sub>2</sub>O<sub>3</sub>); O: Olivine ((Mg,Fe,Ni)<sub>2</sub>SiO<sub>4</sub>)]

#### 4. Conclusions

Palm kernel shell charcoal is the potential to be utilized as a reductant in the saprolite roasting process. The saprolite sample mixed with palm kernel shell charcoal can yield the

identical mineral phase to the sample that used anthracite coal after the roasting process, namely Magnetite, Olivine, and Hematite. The product minerals are transformed from Goethite, confirming the reduction in all samples. In addition, higher temperature and prolonged reduction process increase the conversion of Goethite into magnetite. In terms of kinetics results, the Jander model fits better for both reductants than the Ginstling-Brounshtein model, with lower energy activation for the biomass-based reductant of 10.99 – 18.19 kJ/mol compared to that of anthracite reductant of about 33.68 kJ/mol. The positive results of biomass-based charcoal utilization hopefully encourage the development of a sustainable pyro-based nickel laterite processing process.

### Acknowledgements

We highly appreciate the Ministry of Research, Technology and Higher Education of Indonesia for the financial support in the scheme of PUP (Penelitian Unggulan Perguruan Tinggi) 2364/UN1.P.III/DIT-LIT/LT/2017 and BPDP Kelapa Sawit Research Grant for Students. On behalf of all authors, the corresponding author states that there is no conflict of interest.

### References

- Chen, G., Hwang, W., Liu, S., Shiau, J., 2015. The Effect of Bio-Coal on the on the Carbothermic Reduction of Laterite 'Ores', *Materials Transactions*, Volume 56(4), pp. 550–555
- Citrawati, F., Dwiwandono, R., Firmansyah, L. 2020. The Effect of Ni on the Formation of Bainite in Fe-Ni Lateritic Steels Through Semi-Continuous Cooling Method. *International Journal of Technology*, Volume 11(1), pp. 60–70
- Dalvi, A.D., Bacon, W.G., Osborne, R.C., 2004. The Past and the Future of Nickel Laterites World's Land Based Nickel Resources and Primary Nickel Production Nickel Production. kt / 'yr', *PDAC 2004 International Convention*, pp. 1–27
- Elias, M., 2002. Nickel Laterite Deposits–Geological Overview, Resources and Exploitation. Centre for Ore Deposit Research, University of Tasmania, Special Publication, pp. 205–220
- Fu, J.X., Zhang, C., Hwang, W., Liu, Y., Lin, Y., 2012. Exploration of Biomass Char for CO<sub>2</sub> Reduction in RHF Process For Steel Production. *International Journal of Greenhouse Gas Control*, Volume 8, pp. 143–149
- Guo, X., Li, D., Park, K., Tian, Q., Wu, Z., 2009. Leaching Behavior of Metals from a Limonitic Nickel Laterite using a Sulfation-Roasting-Leaching Process. *Hydrometallurgy*, Volume 99(3–4), pp. 144–150
- Kartohardjono, S., Pamitran, A.S., Putra, N., 2019. Biomass: from Waste to Valuable Materials. *International Journal of Technology*, Volume 10(8), pp. 1465–1468
- Khawam, A., Flanagan, D.R., 2006. Solid-State Kinetic Models: Basics and Mathematical Fundamentals. *Journal of Physical Chemistry B*, Volume 110(35), pp. 17315–17328
- Kim, J., Dodbiba, G., Tanno, H., Okaya, K., Matsuo, S., Fujita, T., 2010. Calcination of Low-Grade Laterite for Concentration of Ni by Magnetic Separation. *Minerals Engineering*, Volume 23(4), pp. 282–288
- Lee, H.Y., Kim, S.G., Oh, J.K., 2005. Electrochemical Leaching of Nickel from Low-Grade Laterites. *Hydrometallurgy*, Volume 77(3–4), pp. 263–268
- Li, B., Wang, H., Wei, Y., 2011. The Reduction of Nickel from Low-Grade Nickel Laterite Ore using a Solid-State Deoxidisation Method. *Minerals Engineering*, Volume 24(14), pp. 1556–1562
- Li, Y.J., Sun, Y., Han, Y., Gao, Y., 2013. Coal-Based Reduction Mechanism of Low-Grade

Laterite Ore. *Transactions of Nonferrous Metals Society of China*, Volume 23(11), pp. 3428–3433

Minister of Energy and Mineral Resources Republic Of Indonesia, 2013. Regulation Of The Minister Of Energy And Mineral Resources Republic Of Indonesia No 20. Indonesia. Available online at [http://jdih.esdm.go.id/Peraturan/Permen ESDM 20 2013. pdf](http://jdih.esdm.go.id/Peraturan/Permen%20ESDM%202013.pdf).

Mondal, K., Lorethova, H., Hippo, E., Wiltowski, T., Lalvani, S.B., 2004. Reduction of Iron Oxide in Carbon Monoxide Atmosphere-Reaction Controlled Kinetics. *Fuel Processing Technology*, Volume 86(1), pp. 33–47

Oediyani, S., Willyandhika, K., Suharto. 2016. The Effect of Reduction Time and Size Distribution of Mixed Iron Ore with Coconut Shell Charcoal on the Percentage Of Metallization by using a Rotary Kiln. *International Journal of Technology*, Volume 7(3), pp. 366–373

Petrus, H.T.B.M., Rhamdani, A.R., Putera, A.D.P., Warmada, I.W., Yuliansyad, A.T., Perdana, I., 2016. Kinetics Study of Carbon Raiser on the Reduction of Nickel Laterite from Pomalaa, Southeast Sulawesi. In: IOP Conference Series: Materials Science and Engineering, Volume 162, Second International Conference on Chemical Engineering (ICCE) UNPAR 26–27 October 2016, Bandung, Indonesia

Petrus, H.T.B.M., Putera, A.D.P., Rhamadani, A., Warmada, I.W., Yuliansyad, A.T., Perdana, I., 2017. Lamtoro Charcoal (*L. Leucocephala*) as Bioreductor in Nickel Laterite Reduction: Performance and Kinetics Study. In: 2nd International Symposium on Frontier of Applied Physics (ISFAP 2016) 3–5 October 2016, Jakarta, Indonesia

Petrus, H.T.B.M., Putera, A.D.P., Sugiarto, E., Perdana, I., Warmada, I.W., Nurjaman, F., Astuti, W., Mursito, A.T., 2019. Kinetics on Roasting Reduction of Limonitic Laterite Ore using Coconut-Charcoal and Anthracite Reductants. *Minerals Engineering*, Volume 132(2), pp. 126–133

Putera, A.D.P., Sugiarto, E., Sutijan, Warmada, I.W., Petrus, H.T.B.M., 2017. Coconut Shell Charcoal as a Bioreductor in Roasting Process of Nickel Laterite from Pomalaa, Southeast Sulawesi: Performance and Kinetics Study. *Materials Science Forum*, Volume 901, pp. 182–189

Rasyid, M.H. Al., Rhamdani, A.R., Putera, A.D.P., Petrus, H.T.B.M., 2016. Study on Biomass Performance in Reduction of Nickel Laterite from Pomalaa, Sulawesi Tenggara. In: AIP Conference Proceedings 1755, p. 050007

Rhamdhani, M.A., Hayes, P.C., Jak, E., 2009. Nickel Laterite Part 1-Microstructure and Phase Characterisations During Reduction Roasting and Leaching. *Transactions of the Institutions of Mining and Metallurgy, Section C: Mineral Processing and Extractive Metallurgy*, 118(3), pp. 129–145

Ribeiro, P.P.M., Neumann, R., Santos, I.D.D., Rezende, M.C., Radino-Rouse, P., Dutra, A.J.B., 2019. Nickel Carriers in Laterite Ores and Their Influence on the Mechanism of Nickel Extraction by Sulfation-Roasting-Leaching Process. *Minerals Engineering*, 131, pp. 90–97

U.S. Geological Survey, 2014. Mineral Commodity Summaries 2014: U.S. Report, Geological Survey, USA

Whittington, B.I. Muir, D., 2000. Pressure Acid Leaching of Nickel Laterites: A Review. *Mineral Processing and Extractive Metallurgy Review*, Volume 21(6), pp. 527–599

Yunus, N.A., Ani, M.H., Salleh, H.M., Rashid, R.Z.A., Akiyama, T., Purwanto, H., Othman, N.E.F., 2014. Effect of Reduction Roasting by using Biochar Derived from Empty Fruit Bunch on the Magnetic Properties of Malaysian Iron Ore. *International Journal of Minerals, Metallurgy and Materials*, Volume 21(4), pp. 326–330